

SIMULATION OF SWITCHING ARCS IN CLIMATE-NEUTRAL 420 KV EARTHING SWITCHES AND DISCONNECTORS FILLED WITH CLEAN AIR

F. REICHERT*, A. PETCHANKA, P. G. NIKOLIC, A. GRIEGER

Siemens Energy, Paulsternstr. 26, 13629 Berlin, Germany

* frank.reichert@siemens-energy.com

Abstract. This contribution focusses on the modelling and simulation of switching arcs in the active back parts of a Clean Air-filled gas-insulated switchgear, namely the high-speed earthing switch and the disconnector. Two simulation approaches are presented. The first presented arc model uses the conventional 2D axisymmetric workflow based on the assumption of the conservation of electrical current. In contrast, the second presented arc model uses an alternative 2D axisymmetric simulation approach where the arc size is conserved by means of a scaling of the arc current. This approach allows the simulation of the electrical arc located away from the geometrical rotational symmetry axis. The simulation results are in good agreement to the measurements in a real earthing switch and in a real disconnector, respectively, thus validating the simulation approaches.

Keywords: gas-insulated switchgear, Clean Air, CFD arc simulation, modelling, validation.

1. Introduction

Currently, the investigation of various SF₆-alternatives is even more in the focus of science's and industry's current research and development efforts, due to the discussion about a phase-out of sulphur hexafluoride (SF₆) as insulating and arc quenching gas in high-voltage switchgear applications for new installations within the next years. In this context, gas-insulated switchgear with Clean Air (80% N₂ and 20% O₂) insulation and the use of vacuum switching technology for the circuit breaker represent an environment-friendly (GWP = 0) and highly performant SF₆-free solution for future high-voltage switchgear applications.

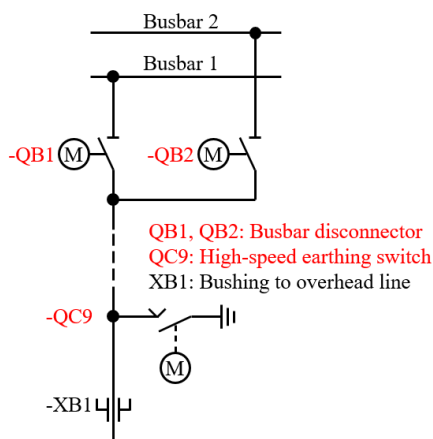


Figure 1. Part of a real single line diagram of a 420 kV gas-insulated switchgear

Within this framework, this contribution focusses on the modelling and simulation of switching arcs in the active back parts of a Clean Air-filled gas-insulated switchgear, namely the high-speed earthing switch and the disconnector. Figure 1 highlights the localisation

of these back parts in a typical single line diagram of a 420 kV gas-insulated switchgear.

The busbar disconnectors operate during bus transfers and have to switch-off bus-transfer currents in the dimension of several thousand amperes. Depending on the considered loop length (impedance ratio of paths), a bus-transfer voltage appears across the open disconnector terminals. The standard IEC 62271-102 defines for the regarded voltage level $245 \text{ kV} \leq U_r \leq 550 \text{ kV}$ a test current of $I_{\text{test,rms}} = 3000 \text{ A}$ and a test voltage of $U_{\text{test,rms}} = 25 \text{ V}$ [1] where rms is the abbreviation for root mean square.

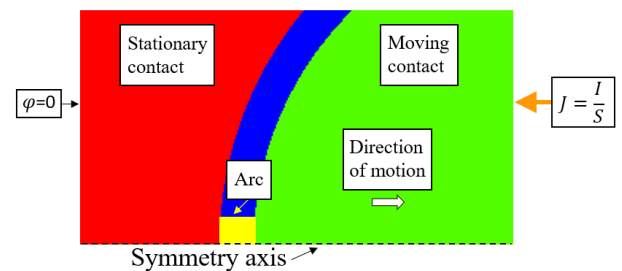


Figure 2. Part of solution domain with boundary conditions for the busbar disconnector geometry

Figure 2 shows a part of the solution domain for the simulation of the switching-off process in the busbar disconnector geometry. As it can be seen from Figure 2, the arc is aligned along the symmetry axis. Thus the conventional 2D axisymmetric arc model based on the assumption of the conservation of electrical current could be used in the simulation.

The high-speed earthing switch has to deal with induced currents in de-energized lines as a result of inductive and capacitive coupling with adjacent energized lines [2]. The high-speed earthing switch has to

interrupt an inductive current when the de-energized line is earthed at one termination and earthing switching is performed at the other termination, see Figure 3.

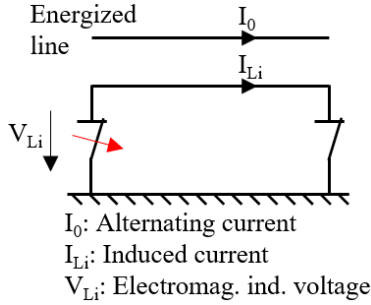


Figure 3. Equivalent circuit diagram in case of inductive switching [2]

The high-speed earthing switch has to interrupt a capacitive current when the earth connection is open at one termination and earthing switching is performed at the other termination, see Figure 4.

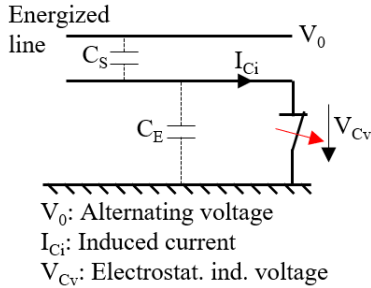


Figure 4. Equivalent circuit diagram in case of capacitive switching [2]

In this contribution, the inductive switching is only regarded. The corresponding test duty defined by IEC 62271-102 for $U_r = 420$ kV comprises a test current of $I_{test,rms} = 160$ A and a test voltage of $U_{test,rms} = 10$ kV [1]. Figure 5 shows a part of the solution domain for the simulation of the switching-off process in the high-speed earthing switch geometry.

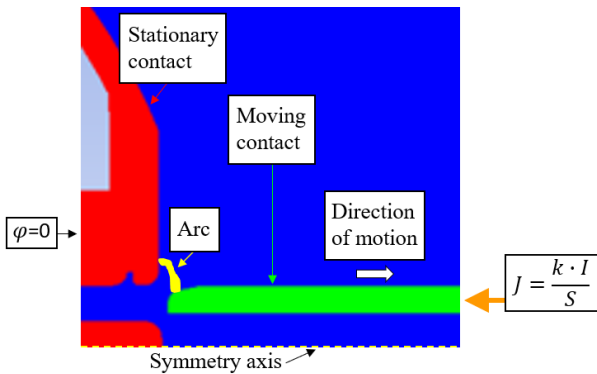


Figure 5. Part of solution domain with boundary conditions for the high-speed earthing switch geometry

The assumption of the arc current conservation works properly only in case of the same arc rotational

symmetry axis for the considered arc configuration and for the simulation domain. If this is not the case, as it is presented in Figure 5 for the high-speed earthing switch geometry, the change of the inner arc structure becomes noticeable. Such considerable change results in an unphysical arc configuration with a drastic modification of the arc dynamics (arc voltage, heat transfer, radiation losses, temperature distribution etc.). Thus in the simulation of the switching-off process in the high-speed earthing switch geometry, the alternative simulation approach presented in [3] has been used where the conservation of the arc size instead of the arc current at the transition from 3D to 2D axi-symmetrical geometry is considered. The arc model derived under such assumption has resulted in a good agreement to the measurements, good numerical stability and affordable numerical costs.

2. Modelling and simulation

2.1. Simulation tool for pure Clean Air

The numerical simulation and thus the description of the fluid mechanical processes in both regarded geometries during the switching-off process is carried out using a modular simulation model which is based on the CFD program ANSYS/FLUENT. Figure 6 shows the set-up of the simulation model. Clean Air is considered as the quenching gas. Thermodynamic and transport properties of hot Clean Air are modeled by means of a Real Gas Model based on the tabulated values of the gas properties in dependence on pressure and temperature. The material properties of the solid electrodes are taken into account in dependence on the temperature.

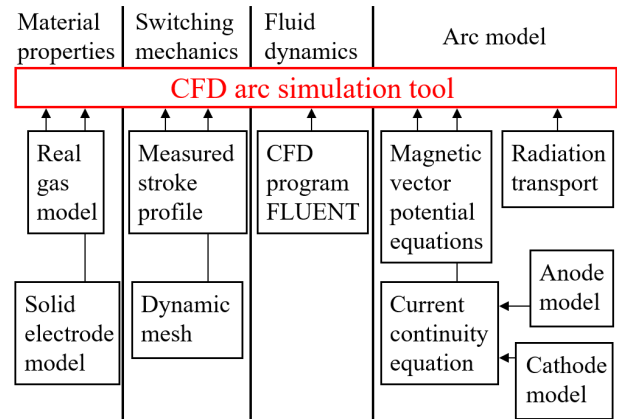


Figure 6. CFD arc simulation tool structure

The contact motion is implemented in the CFD arc simulation tool based on ANSYS/Fluent software by means of dynamic mesh. The arc models are based on the solution of the Navier-Stokes equations for hot gas flow, the non-gray multiband Discrete Ordinate Model (DOM) for the radiation transport, the current continuity equation for the electrical current transfer and the magnetic vector potential equations for the magnetic field distribution. Typical boundary conditions

for the current continuity equation are the uniform current density corresponding to the interruption current at the current input and zero potential at the current output, see e.g. Figure 2. The electrode-fluid interfaces are realized by models for the anode and the cathode, respectively [4]. For the magnetic vector potential equations boundary conditions according to [5] have been used.

2.2. Particularities of alternative arc model

According to Figure 7a and Figure 7b, the variation of the arc size (e.g. at arc attachment) at the transition from 3D to 2D axi-symmetrical geometry under the assumption of the arc current conservation can be easily evaluated by using the following assumption:

$$I = \pi R_{\text{arc}}^2 J \approx 2\pi r d J = I_{2D}. \quad (1)$$

In eq. 1, I is the arc current in 3D geometry, R_{arc} is the arc radius in 3D geometry, r is the distance from the symmetry axis, J is the effective current density which supposed to be nearly the same both in 3D and 2D configuration and d is the arc width in case of 2D axi-symmetrical geometry. Eq. 1 transposed to d gives:

$$d = \frac{R_{\text{arc}}^2}{2r}. \quad (2)$$

For large distances between the symmetry axis and

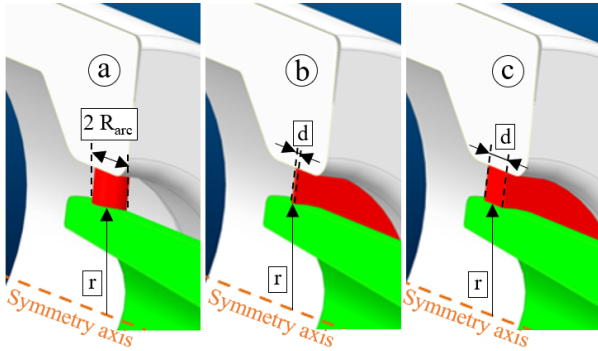


Figure 7. Illustration of different arc configurations (a: 3D arc, b: 2D arc, c: Alternative 2D arc)

the arc follows the inequality $r \gg R_{\text{arc}}$ and $d \ll R_{\text{arc}}$. This leads to a drastic modification of the simulated arc dynamics (arc voltage, heat transfer, radiation losses, temperature distribution etc.) and numerical issues.

As mentioned, the presented arc model uses an alternative 2D axi-symmetrical simulation approach. In this approach the arc size is conserved under the assumption of the same current density. In doing so, the arc current in case of 2D axi-symmetrical geometry I_{2D} is scaled in respect of the actual arc current in the 3D geometry I as follows

$$I_{2D} = kI, \quad (3)$$

where k is the scaling factor. The arc configuration corresponding to the alternative 2D axi-symmetrical

simulation approach is presented in Figure 7c. The value of k is chosen to keep the same current density and the same arc thickness in 2D as in the original 3D configuration:

$$d = 2R_{\text{arc}}. \quad (4)$$

Using eq. 3 and eq. 4, the scaling factor k can be evaluated as follows:

$$\frac{I}{\pi R_{\text{arc}}^2} = \frac{kI}{4\pi r R_{\text{arc}}} \implies k = \frac{4r}{R_{\text{arc}}}. \quad (5)$$

The value for R_{arc} is pre-calculated by means of the conventional 2D axisymmetric arc model with the interruption current I in a rectangular simulation domain where the simulation domain axis and the arc axis coincides, see Figure 8.

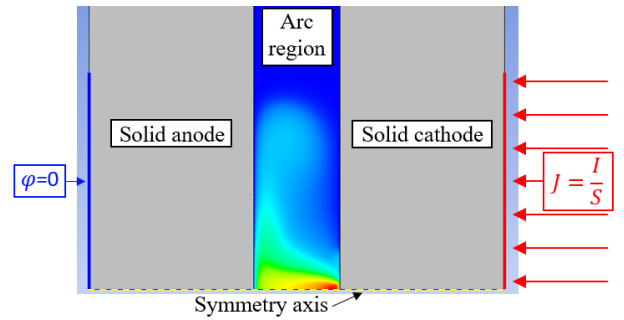


Figure 8. Visualization of the simulation model for the calculation of R_{arc}

The scaling factor can be either a function of the radial coordinate as in [6] or a constant value. In this contribution, the scaling factor is constant and corresponds to a characteristic radius of the regarded high-speed earthing switch geometry.

2.3. Extension with respect to electrode evaporation

At higher interrupting currents (kA range), it can be necessary to consider the evaporation of electrodes. In this case, the CFD arc simulation tool according to Figure 6 must be extended by a 2 species real gas model in our case for the mixture Clean Air+Copper and an electrode ablation model for the calculation of mass conservation, momentum equations and energy equation [7]. Furthermore, the radiation of the plasma must be treated with mean absorption coefficients for the mixture Clean Air+Copper and an additional conservation equation for the Copper species must be solved.

3. Simulation results

3.1. Switching-off process in the high-speed earthing switch geometry

The presented alternative arc model has been used to simulate the switching-off process in the high-speed earthing switch geometry according to Figure 5 with

respect to the mentioned test duty for inductive switching. The stroke profile and the current trend from Figure 9 has been taken as input quantities for the simulation.

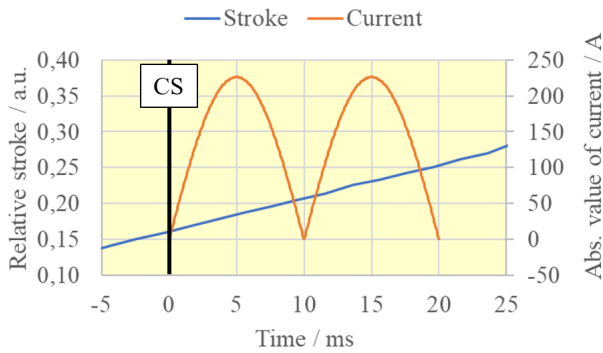


Figure 9. Stroke profile and interruption current (CS: Contact separation)

The knowledge of the response of the switching device on the interrupting current such as the arc voltage can be used to improve its design in the development process. In this context, it is common practice to measure the arc voltage in the tests of the switching device. Figure 10 shows two arc voltage trends which have been measured in the regarded earthing switch during the interruption of the current from Figure 9. As it can be seen from Figure 10, the measured arc voltage increases continuously during the switching-off process. Nevertheless, the presented arc voltage trends show a lot of fluctuations indicating a strong arc dynamics.

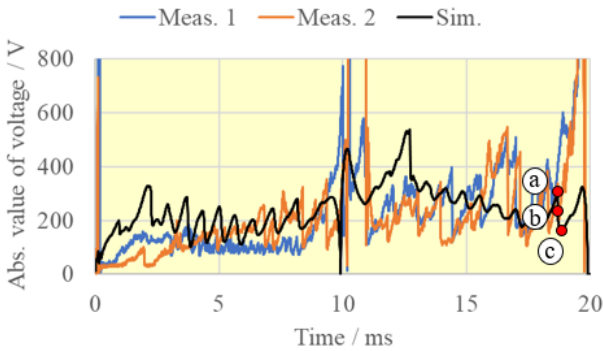


Figure 10. Comparison of measured and simulated arc voltage

This behaviour is confirmed by the CFD arc simulation as it can be seen from the simulated arc voltage which is also depicted in Figure 10. The comparison according to Figure 10 demonstrates a good agreement between measurement and simulation, thus validating the alternative 2D axi-symmetrical simulation approach.

In accordance with the measured trends of arc voltage, the simulated arc voltage trend shows phases where the arc voltage increases continuously and phases with a lot of fluctuations, see e.g. at the time instants a to c in Figure 10.

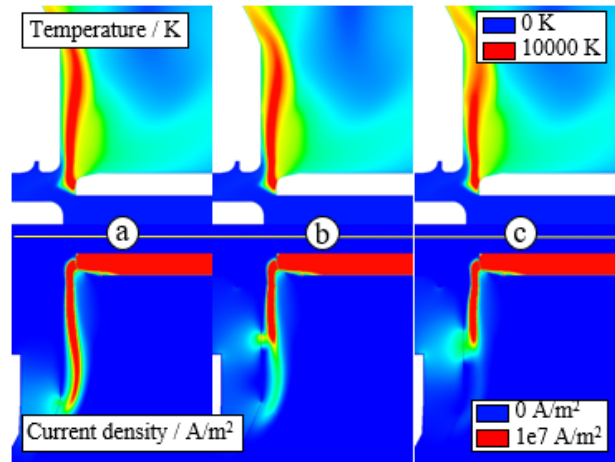


Figure 11. Distribution of temperature and current density at different time instants

This behaviour is the result of a serial elongation and shortening of the arc. The presented CFD arc simulation tool is able to reflect this effect as it can be seen from Figure 11. The arc attachment at the moving contact is more or less fixed. In contrast to this behaviour, the arc attachment at the stationary contact is not fixed and changes its radial position from time instant a to time instant c which leads to strong variations of arc voltage.

3.2. Consideration of Copper vapour

The conventional 2D axisymmetric arc model with arc aligned along the axis and with extension for the consideration of electrode evaporation has been used to simulate the switching-off process in the busbar disconnector geometry with respect to the mentioned test duty for bus transfer.

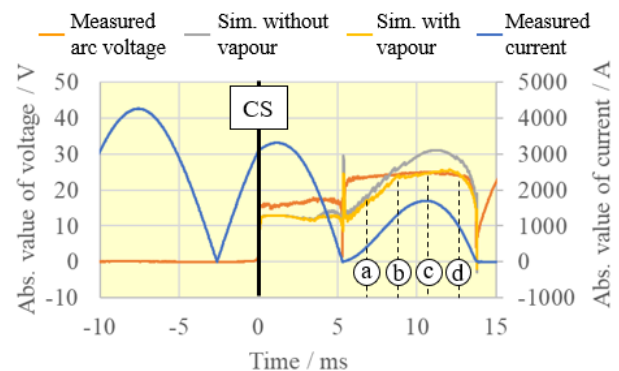


Figure 12. Comparison of measured and simulated signals with respect to test duty for bus transfer

As it can be seen from Figure 12, the additional arc voltage in the test circuit forces a current limitation just after contact separation (CS) and the current tends to zero at the end of the last current half wave.

The switching-off process in the disconnector geometry has been simulated with and without consideration of copper vapour. Figure 12 highlights the influence of the Copper vapour on the simulated arc voltage,

too. During the last current half wave, the differences between both simulated curves increases by the strong metal vapour production. This behaviour is clarified by the distributions of Copper mass fractions in Figure 13 indicating the increasing vapour production over time. It can be noted that the electrode evaporation should be considered in simulations with an interruption current of several kA.

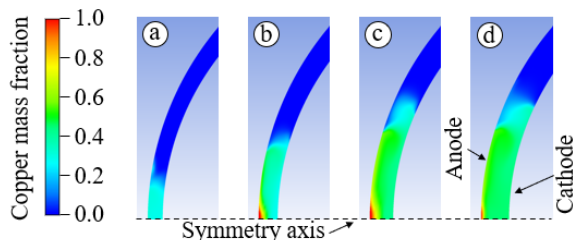


Figure 13. Mass fraction distribution at different time instants

The comparison according to Figure 12 demonstrates a good agreement between measured and simulated arc voltages, thus validating the conventional 2D axi-symmetrical simulation approach.

4. Conclusions

The contribution deals with the switching-off process in the active back parts of a Clean Air-filled gas-insulated switchgear.

Two simulation approaches for the CFD arc simulation in 2D axi-symmetrical solution domains has been presented.

The alternative arc model based on the conservation of arc size has been used to simulate the switching-off process in a real high-speed earthing switch configuration. The simulated arc voltage is in good agreement to the measurements and reproduces properly the important features of the arc dynamics such as elongation and shortening. In the simulation using this alternative arc model, the arc takes the shape of a hollow disk and occupies more volume than the corresponding arc in reality or 3D simulation. This effect can result in deviations e.g. concerning the pressure build-up in the arc volume and the temperature distribution in the arc column. Thus, it is necessary to generate additional data for the validation of the alternative arc model in further investigations by measurements and/or 3D simulations.

The conventional 2D axisymmetric arc model with arc aligned along the axis has been used to simulate the switching-off process in a busbar disconnector configuration taking into account the electrode evaporation or not. It could be shown that the effect of the electrode evaporation must be considered for an interruption current of several kA.

The presented CFD arc simulation tool offers the capability to support the development process of the active back parts of Clean Air-filled gas-insulated switchgears.

Acknowledgements

The authors are grateful to Pierre Freton, Jean-Jacques Gonzalez, Yann Cressault and Philippe Teulet from the University Paul Sabatier in Toulouse for their support and participation in the developments of numerous sub-models and for providing of thermodynamic, transport and radiation properties.

Parts of the research work were supported by the German Federal Ministry for Economic Affairs and Climate Action.

Supported by:



on the basis of a decision
by the German Bundestag

References

- [1] IEC 62271-102 High-voltage switchgear and controlgear – Part 102: Alternating current disconnectors and earthing switches.
- [2] CIGRE, Technical Brochures, 570, WG A3.28, 2014, Switching Phenomena for EHV and UHV Equipment.
- [3] A. Petchanka and F. Reichert. CFD Simulation of a 3D Featured Electrical Arc Configuration in a 2D Axisymmetrical Simulation Domain. *Proceedings of 22nd International Conference on Gas Discharges and their Applications*, pages 95–98, 2018.
- [4] F. Lago, J. J. Gonzalez, P. Freton, and A. Gleizes. A numerical modelling of an electric arc and its interaction with the anode: Part i. the two-dimensional model. *J. Phys. D: Appl. Phys.*, 37(6):883, 2004. doi:10.1088/0022-3727/37/6/013.
- [5] P. Freton, J. J. Gonzalez, M. Masquère, and F. Reichert. Magnetic field approaches in dc thermal plasma modelling. *J. Phys. D: Appl. Phys.*, 44(34):345202, 2011. doi:10.1088/0022-3727/44/34/345202.
- [6] A. Petchanka and F. Reichert. CFD Arc Simulation of HVDC Circuit-Breakers. *Proceedings of 23rd International Conference on Gas Discharges and their Applications*, pages 56–59, 2023.
- [7] P. Freton et al. Influence of copper vapours in SF₆ plasma. *Plasma Physics and Technology*, 6(2):161–164, 2019. doi:doi:10.14311/ppt.2019.2.161.